MULTISECTIONS OF SURFACE BUNDLES AND BUNDLES OVER S^1

Delphine Moussard

Abstract: A multisection is a decomposition of a manifold into 1-handlebodies, where each subcollection of the pieces intersects along a 1-handlebody except the global intersection, which is a closed surface. These generalizations of Heegaard splittings and Gay–Kirby trisections were introduced by Ben Aribi, Courte, Golla, and the author, who proved in particular that any 5-manifold admits such a multisection. In arbitrary dimension, we show that two classes of manifolds admit multisections: surface bundles and fiber bundles over the circle, whose fiber itself is multisected. We provide explicit constructions, with examples.

1. Introduction

Heegaard splittings are standard decompositions of closed orientable 3-manifolds into two handlebodies. In [**2**], Gay and Kirby introduced analogous decompositions of 4-manifolds, the so-called trisections; they proved that all closed orientable smooth 4-manifolds admit such trisections. More recently, in [**1**], Ben Aribi, Courte, Golla, and the author studied a notion of multisection for closed orientable manifolds of any dimension, which encompasses Heegaard splittings and trisections: a multisection of an $(n+1)$-manifold is a decomposition into n 1-handlebodies such that each subcollection intersects along a 1-handlebody, except the global intersection, which is a closed surface. They proved in particular that any smooth 5-manifold admits a multisection. Here, we study the existence of multisections in arbitrary dimension for two classes of manifolds: surface bundles and bundles over the circle. This generalizes works on 4-manifolds by Williams [**8**] for surface bundles and by Koenig [**5**] for bundles over the circle.

Theorem (Theorem 3.2). *Any surface bundle admits a multisection.*

Theorem (Theorem 4.1). *Any fiber bundle over S^1 whose fiber admits a multisection globally preserved by the monodromy (ie permuting the pieces of the multisection) admits a multisection.*

The proofs are constructive. We show how to get a multisection diagram of the bundle, either from a suitable decomposition of the base in the case of surface bundles, or from a multisection diagram of the fiber in the case of bundles over S^1.

As noted by Koenig in [**5**], for a 4-dimensional fiber bundle over S^1, the fiber always admits a Heegaard splitting preserved by the monodromy: if $\mathcal{H}$ is a given Heegaard splitting of the fiber and φ is the monodromy, then, by uniqueness of Heegaard split-

tings, $\mathcal{H}$ and $\varphi(\mathcal{H})$ have a common stabilization; this stabilization of $\mathcal{H}$ is preserved by the monodromy. This argument applies to 5-dimensional fiber bundles over S^1, because a given 4-manifold (here, the fiber) always admits a trisection, which is unique up to stabilization [2]. In higher dimensions, however, the question of uniqueness up to stabilization of the multisections is open.

It may be worth mentioning that other notions of multisections do exist, that should not be confused with the ones we consider here. In [7], Rubinstein and Tillmann defined multisections of PL manifolds, which coincide with Heegaard splittings in dimension 3 and with trisections in dimension 4. In higher dimensions, however, these multisections differ from ours; in particular they cannot be represented by diagrams. Also, in [3], Islambouli and Naylor introduced multisections of 4-dimensional manifolds, which generalize trisections to decompositions with an arbitrary number of pieces.

Throughout the article, all manifolds are orientable. We work in the PL category, but our constructions of multisections also work in the smooth category, *ie* with smooth manifolds and smooth multisections; see Remark 2.1. The only result which does not adapt to the smooth setting in all dimensions is Proposition 2.2 and this is clarified at that point.

2. Multisections and diagrams

For $n \geq 3$, an *n-dimensional handlebody* is a manifold that admits a handle decomposition with one 0-handle and some 1-handles; the number of 1-handles is the *genus* of the handlebody.

A *multisection*, or *n-section*, of a closed connected $(n+1)$-manifold W is a decomposition $W = \bigcup_{i=1}^n W_i$ where:

- for any non-empty proper subset I of $\{1,\ldots,n\}$, the intersection $W_I = \bigcap_{i \in I} W_i$ is a submanifold of W which is PL-homeomorphic to an $(n-|I|+2)$-dimensional handlebody,
- $\Sigma = \bigcap_{i=1}^n W_i$ is a closed connected surface.

A multisection is a *Heegaard splitting* when $n = 2$, a *trisection* when $n = 3$, a *quadrisection* when $n = 4$. The *genus* of the multisection is the genus of the *central surface* Σ.

Remark 2.1. In the smooth category, the W_I cannot all be smooth submanifolds of W: some corners necessarily appear. This forces us to give a more detailed definition; see [1].

Given a 3-dimensional handlebody H with boundary Σ, a *cut system* for H is a collection of disjoint simple closed curves on Σ which bound disjoint properly embedded disks in H such that the result of cutting H along these disks is a 3-ball. Recall that a cut system is well defined up to handleslides [4, Corollary 1.6]. A *multisection diagram* for a multisection as above is a tuple $(\Sigma; (c_i)_{1 \leq i \leq n})$, where Σ is the central surface of the multisection and c_i is a cut system on Σ for the 3-dimensional handlebody $\bigcap_{j \neq i} W_j$. By [1, Theorem 3.2], a multisection diagram determines a unique PL manifold (and a unique smooth manifold up to dimension 6).

The connected sum of multisected manifolds can be performed around points of the central surfaces, so as to produce a multisection of the resulting manifold. This gives a simple way to define stabilizations of multisections: a *stabilization* of a multisection of an $(n+1)$-manifold W is the connected sum of the multisected W with the standard

sphere S^{n+1} equipped with a genus-1 multisection; the latter are given diagrammatically in Figure 1. These stabilization moves can also be described as cut-and-paste operations on the multisection of W; see [**1**].
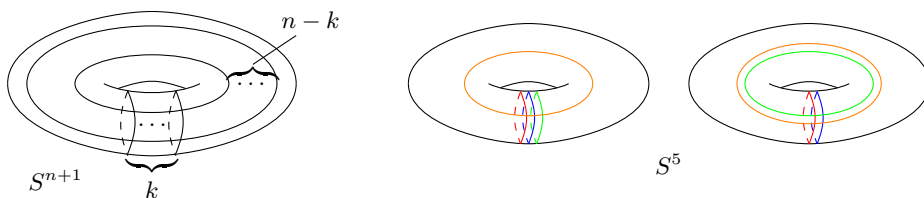

FIGURE 1. Genus-1 multisection diagrams of the spheres, where $0 < k < n$.

Proposition 2.2. *Let W be an $(n + 1)$-manifold with a multisection diagram $(\Sigma; (c_i)_{1 \leq i \leq n})$. Assume the diagram contains two groups of k and $n-k$ parallel curves, with $0 < k < n$, such that a curve of one group meets a curve of the other group in exactly one point. Then the associated multisection is the result of a stabilization.*

Proof: Denote by $\alpha_1, \ldots, \alpha_k$ and $\beta_{k+1}, \ldots, \beta_n$ the two groups of curves. Since two curves in the same collection c_i have to be disjoint but not parallel, there is one of these curves in each c_i. If a curve of the diagram, other than the β-curves, meets the α-curves, then it is in the same collection c_i as one of the β-curves, so that it can be slid along this β-curve until it gets disjoint from the α-curves. The same is true for a curve, other than the α-curves, that would meet the β-curves. Hence, after handleslides, we can assume that the α-curves and the β-curves are disjoint from any other curve of the diagram. Now a regular neighborhood of the α-curves and the β-curves in Σ is a punctured torus. It implies that the diagram is a connected sum of a lower-genus diagram with a diagram of Figure 1. Since the multisected manifold is determined by the diagram, it is the result of a stabilization. $\qquad\square$

We will use this proposition in Section 4 to simplify some multisection diagrams. We may note that, for a smooth manifold, this proof works up to dimension 6 only: the point is that a multisection diagram determines a unique smooth manifold up to dimension 6 only, so that the last sentence of the proof does not apply in higher dimensions.

3. Multisecting surface bundles

Surface bundles turn out to admit multisections in any dimension. A multisection of a surface bundle can be obtained from a suitable decomposition of the base into balls. This generalizes the work of Gay–Kirby [**2**] and Williams [**8**] on trisections of 4-dimensional surface bundles.

Let M be a closed d-manifold. We call *good ball decomposition* of the manifold M a decomposition $M = \bigcup_{i=0}^{d} M_i$ where, for all non-empty $I \subset \{0, \ldots, d\}$, $\bigcap_{i \in I} M_i$ is a disjoint union of embedded $(d - |I| + 1)$-balls. Such decompositions do exist.

Lemma 3.1. *Any closed manifold admits a good ball decomposition.*

Proof: Let M be a closed d-manifold and $\mathcal{T}$ a triangulation of M. We consider the first and second barycentric subdivisions $\mathcal{T}^1$ and $\mathcal{T}^2$ of $\mathcal{T}$. For $i \in \{0, \ldots, d\}$, let V_i be the set of barycenters of i-faces of $\mathcal{T}$; note that the union of the V_i is the set of vertices of $\mathcal{T}^1$. We define M_i as the union of the stars of the vertices of V_i in $\mathcal{T}^2$; see

Figure 2. We may note that M_i is the union of i-handles in the handle decomposition of M associated with the triangulation $\mathcal{T}$ (see for instance [**6**, Proposition 6.9]). The condition on the intersections is direct. $\qquad\square$
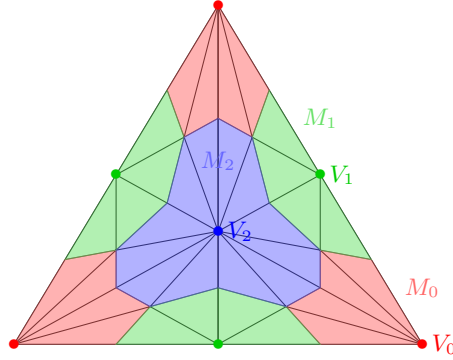

FIGURE 2. For $d = 2$, decomposition of a 2-simplex into the M_i.

Let $p \colon W \to M$ be a surface bundle. Taking the preimage of a good ball decomposition of M, we get a decomposition of W into pieces that are products of a surface, the fiber, with balls. To obtain a multisection from this, we dig some "disk tunnels" into the different pieces, which we add to other pieces. If $N \subset M$ is a disjoint union of contractible subspaces of M, a *disk section of p over N* is a submanifold Z of W such that $p^{-1}(x) \cap Z$ is a 2-disk for all $x \in N$, and $p(Z) = N$.

Theorem 3.2. *Fix $n > 1$. Let $p \colon W \to M$ be a surface bundle, where W is a closed $(n + 1)$-manifold. Assume we are given a good ball decomposition $M = \bigcup_{i=1}^n M_i$. Fix pairwise disjoint disk sections Z_i of p over M_i, for $1 \leq i \leq n$. Set $W_i = \overline{(p^{-1}(M_i) \setminus Z_i)} \cup Z_{i+1}$, where the indices are considered modulo n. Then $W = \bigcup_{i=1}^n W_i$ is a multisection.*

Proof: Set $M_I = \bigcap_{i \in I} M_i$. We slightly abuse notation by denoting $Z_i = M_i \times D_i$, where D_i is a disk in the fiber S above each point of M_i, indeed depending on this point. In this way, W_i can be written as

$$W_i = (M_i \times \overline{S \setminus D_i}) \cup (M_{i+1} \times D_{i+1}).$$

More generally, for $I \subset \{1, \ldots, n\}$, one can check by induction on $|I|$ that:

$$W_I = \left(M_I \times \overline{S \setminus \bigcup_{i \in I} D_i}\right) \cup \bigcup_{\substack{i \in I \\ i+1 \notin I}} (M_{I \cup \{i+1\} \setminus \{i\}} \times D_{i+1}) \cup \bigcup_{\substack{i \in I \\ i+1 \in I}} (M_{I \setminus \{i\}} \times \partial D_{i+1}).$$

We fix a non-empty proper subset I of $\{1, \ldots, n\}$ and check that W_I is a handlebody. In the first term, each connected component is a thickening of a surface with non-empty boundary, thus a handlebody. The second term adds 1-handles to these handlebodies; indeed, M_I and $M_{I \cup \{i+1\} \setminus \{i\}}$ are made of $(n - |I|)$-balls that intersect along $(n-|I|-1)$-balls. For $i \in I$ such that $i+1 \in I$, $M_{I \setminus \{i\}}$ is made of $(n-|I|+1)$-balls and contains in its boundary the $(n-|I|)$-balls composing M_I. Hence each component of $M_{I \setminus \{i\}} \times \partial D_{i+1}$ is a $D^{n-|I|+1} \times S^1$ glued along some $D^{n-|I|} \times S^1$, with $D^{n-|I|}$ living in the boundary of $D^{n-|I|+1}$, to some handlebodies in $M_I \times \overline{S \setminus \bigcup_{i \in I} D_i}$. This has the effect of gluing together some of the latter handlebodies along a 1-handle corresponding to the boundary component ∂D_{i+1} of $\overline{S \setminus \bigcup_{i \in I} D_i}$. Finally, W_I is made of handlebodies and it remains to check that it is connected.

Thanks to the above formula for W_I, it is enough to check that the different connected components of M_I are connected by some number of paths, each contained in $M_{I \cup \{i+1\} \setminus \{i\}}$ (which is contained in $M_{I \setminus \{i\}}$) for some $i \in I$. Note that the connectedness of M implies that $\bigcup_{|I|=n-1} M_I$ is connected (the good ball decomposition provides a CW-complex structure where the k-skeleton is $\bigcup_{|I|=n-k} M_I$). Hence two components of M_I are always connected by a path in $\bigcup_{|I|=n-1} M_I$, and each interval of this path which is not in M_I is a component of $M_{\{1,\ldots,n\} \setminus \{i\}}$ for some $i \in I$, which is contained in $M_{I \cup \{i+1\} \setminus \{i\}}$.

Finally, the central piece $\Sigma = W_{\{1,\ldots,n\}}$ is given by

$$\Sigma = \left(M_{\{1,\ldots,n\}} \times \overline{S \setminus \bigcup_{i=1}^{n} D_i} \right) \cup \bigcup_{i=1}^{n} (M_{\{1,\ldots,n\} \setminus \{i\}} \times \partial D_{i+1}).$$

The first term is made of copies of S with the open D_i removed, while the second term is made of tubes joining the boundary components of these copies. Hence Σ is a closed surface. $\qquad \square$

Remark 3.3. The multisection obtained in the theorem has genus $vg + e - v + 1$, where v is the number of points in $M_{\{1,\ldots,n\}}$, e is the number of intervals in $\bigcup_{|I|=n-1} M_I$, and g is the genus of the fiber.

We now present some examples. When the bundle is simply a product, we define the disk sections as $Z_i = M_i \times D_i$, where the D_i are disjoint disks on the fiber.

We start with bundles over spheres. The standard sphere admits the good ball decomposition given by the following lemma; see Figure 3.

Lemma 3.4. *The $(n-1)$-sphere admits a good ball decomposition $S^{n-1} = \bigcup_{i=1}^{n} B_i$ where $\bigcap_{i \in I} B_i$ is a single $(n - |I|)$-ball for $I \subsetneq \{1, \ldots, n\}$ and $\bigcap_{i=1}^{n} B_i$ is made of two points.*

Proof: Consider the map $\varphi \colon S^{n-1} \subset \mathbb{R}^n \to \mathbb{R}^{n-1}$ sending $(x_1, \ldots, x_n)$ to $(x_1, \ldots, x_{n-1})$. Its image B^{n-1} can be viewed as an $(n-1)$-simplex and cut into the cones with vertex its center and bases its faces. The pull-back of this decomposition provides the required decomposition of S^{n-1}. $\qquad \square$
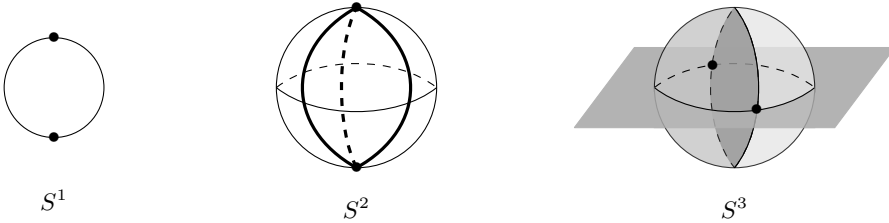

FIGURE 3. Good ball decomposition of S^k for small k.

Corollary 3.5. *A surface bundle over S^{n-1} with fiber a closed surface of genus g admits a multisection of genus $2g + n - 1$.*

If W is a surface bundle over S^{n-1}, the associated multisection has a central surface given by two copies of the fiber (the preimages of $\bigcap_{i=1}^{n} B_i$) joined by a tube above each $\bigcap_{j \neq i} B_j$. Examples of the associated diagram are given in Figures 4 and 5. The

cut system associated to $W_{\{1,\dots,n\}\setminus\{i\}}$ is obtained as follows. A first curve is given by a meridian curve around the tube above $\bigcap_{j\neq i-1} B_j$. Then take a family of properly embedded arcs on $S \setminus \bigcup_{j\neq i} D_j$ that cut it into a disk, and build simple closed curves on Σ by joining the two copies of these arcs on the two copies of the punctured S by parallel arcs on the tubes.
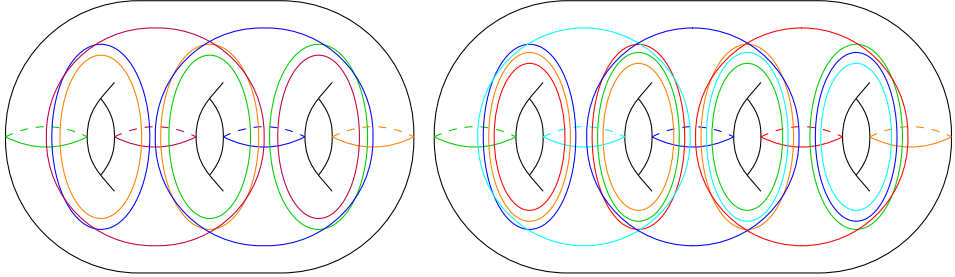

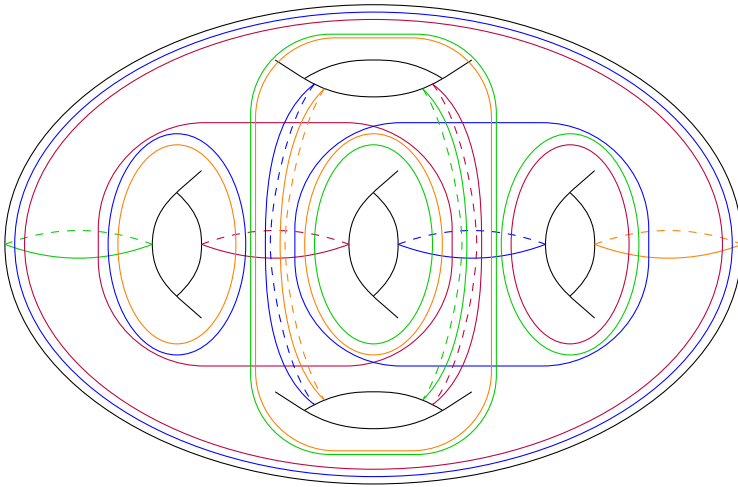FIGURE 4. Multisection diagrams for $S^2 \times S^3$ and $S^2 \times S^4$.

FIGURE 5. Quadrisection diagram for $S^1 \times S^1 \times S^3$.

In dimension 6, we get infinitely many 6-manifolds admitting a 5-section of genus 4, namely the S^2-bundles over S^4. Such a bundle can be constructed by gluing two copies of $S^2 \times B^4$ via a map $\varphi\colon S^3 \to SO(3)$. We write S^3 as the quotient of $S^2 \times [0, 2\pi]$ by the shrinking of $S^2 \times \{0\}$ and $S^2 \times \{2\pi\}$; for $m \in \mathbb{Z}$, we define a map φ_m that sends $(x, t) \in S^2 \times [0, 2\pi]$ onto the rotation of axis given by x and angle mt. This defines an S^2-bundle $W(m)$. While $W(-m)$ is diffeomorphic to $W(m)$, the group $\pi_3(W(m))$ is finite of order $|m|$, which shows that the $W(m)$ for $m \in \mathbb{N}$ are non-diffeomorphic (the order of $\pi_3(W(m))$ can be computed from the homotopy exact sequence of the fibration). To get a simple multisection diagram of $W(m)$, it appears helpful to modify the map φ_m by a homotopy. We write S^3 as $S^2 \times [-1, 2\pi]$ with $S^2 \times \{-1\}$ and $S^2 \times \{2\pi\}$ shrunk, and we define φ_m as previously on $S^2 \times [0, 2\pi]$ and constant equal to the identity on $S^2 \times [-1, 0]$. Taking a good ball decomposition $S^4 = \bigcup_{1 \leq i \leq 5} B_i$

as in Lemma 3.4, we set $B_a = B_1 \cup B_2$ and $B_b = B_3 \cup B_4 \cup B_5$ and we choose the parametrizations of S^3 as the boundary of B_a and B_b so that:

$$S^3 \cap \partial B_1 = (S^2 \times [-1, 0])/\sim$$
$$S^3 \cap \partial B_2 = (S^2 \times [0, 2\pi])/\sim$$

$$S^3 \cap \partial B_3 = (\Delta_3 \times [-1, 2\pi])/\sim$$
$$S^3 \cap \partial B_4 = (\Delta_4 \times [-1, 2\pi])/\sim$$
$$S^3 \cap \partial B_5 = (\Delta_5 \times [-1, 2\pi])/\sim$$

where $S^2 = \Delta_3 \cup \Delta_4 \cup \Delta_5$ is a good ball decomposition of S^2 as in Figure 3. Now the bundle $W(m)$ is given by the gluing of $S^2 \times B_a$ and $S^2 \times B_b$ via the map $\varphi_m \colon \partial B_a = \partial B_b \to SO(3)$. We choose D_1 and D_2 as small neighborhoods of the two points in $\Delta_3 \cap \Delta_4 \cap \Delta_5$, and $D_3 \subset \Delta_4$, $D_4 \subset \Delta_5$, $D_5 \subset \Delta_3$ disjoint from the image of $D_1 \cup D_2$ by all the $\varphi_m(x) \in SO(3)$ acting on S^2. This gives explicit disk sections, and a careful analysis of the gluing locus, where all the 3-dimensional handlebodies of the multisection lie, provides the diagram in Figure 6. The only 3-dimensional piece where the gluing is non-trivial is W_{2345}, represented in green.
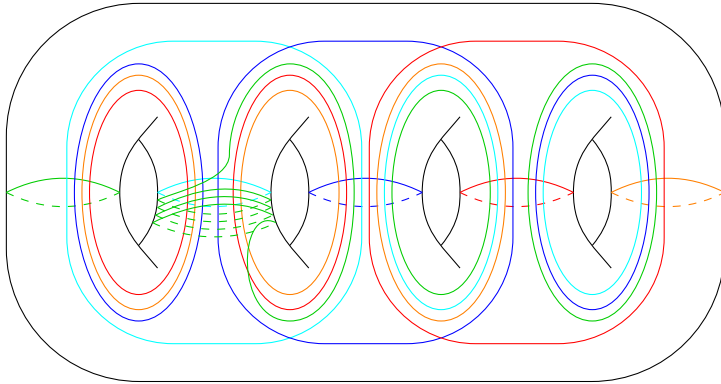

FIGURE 6. Multisection diagram for the S^2-bundle $W(2)$ over S^4.

For a diagram of $W(m)$, the green curve that differs from the diagram of $S^2 \times S^4$ has to turn $2m$ times.

It is an interesting open question to ask whether one can deduce from the diagram that the $W(m)$ are non-diffeomorphic for distinct non-negative values of m.

We now treat surface bundles over $S^2 \times S^1$.

Corollary 3.6. *A surface bundle over $S^2 \times S^1$ admits a quadrisection of genus $8g+9$, where g is the genus of the fiber.*

Proof: We use the following good ball decomposition of $S^2 \times S^1$. The factor S^2 is cut into two disks; each of these disks' product S^1 is then cut into two balls; see Figure 7. In this decomposition $S^2 \times S^1 = \bigcup_{1 \le i \le 4} M_i$, each M_i is a 3-ball, each M_{ij} is made of two 2-disks, each M_{ijk} is made of four intervals, and M_{1234} contains exactly eight points. In the associated quadrisection of a surface bundle over $S^2 \times S^1$, the central surface is made of eight copies of the fiber joined by 16 tubes. $\qquad\square$
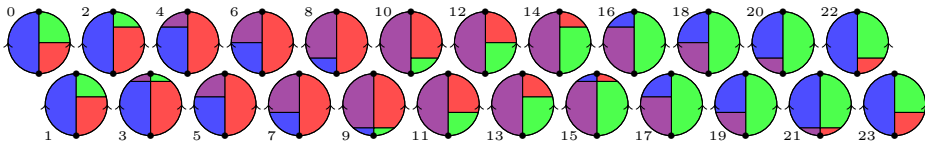

FIGURE 7. Good ball decomposition of $S^2 \times S^1$: the S^2-slices.

Here, S^1 is regarded as $[0, 24]/(0 = 24)$. We represent M_1 in blue, M_2 in violet, M_3 in red, and M_4 in green.

In Figure 8, we give a quadrisection diagram for $S^2 \times S^2 \times S^1$. The surface diagram is the central surface of the quadrisection, made of eight 2-spheres, one above each point of M_{1234}, joined by 16 tubes. The eight points of M_{1234} appear on slices 3, 9, 15, and 21 of Figure 7, two points on each slice, and the corresponding 2-spheres are drawn in Figure 8 at the upper-right, upper-left, lower-left, and lower-right corners respectively. The tubes are given by the $\partial D_j \times M_{j,j+1,j+2}$, where $1 \leq j \leq 4$ and each $M_{j,j+1,j+2}$ is made of four arcs; the tubes corresponding to $j = 1, 2, 3, 4$ are circled by a blue, violet, red, and green meridian respectively in Figure 8.
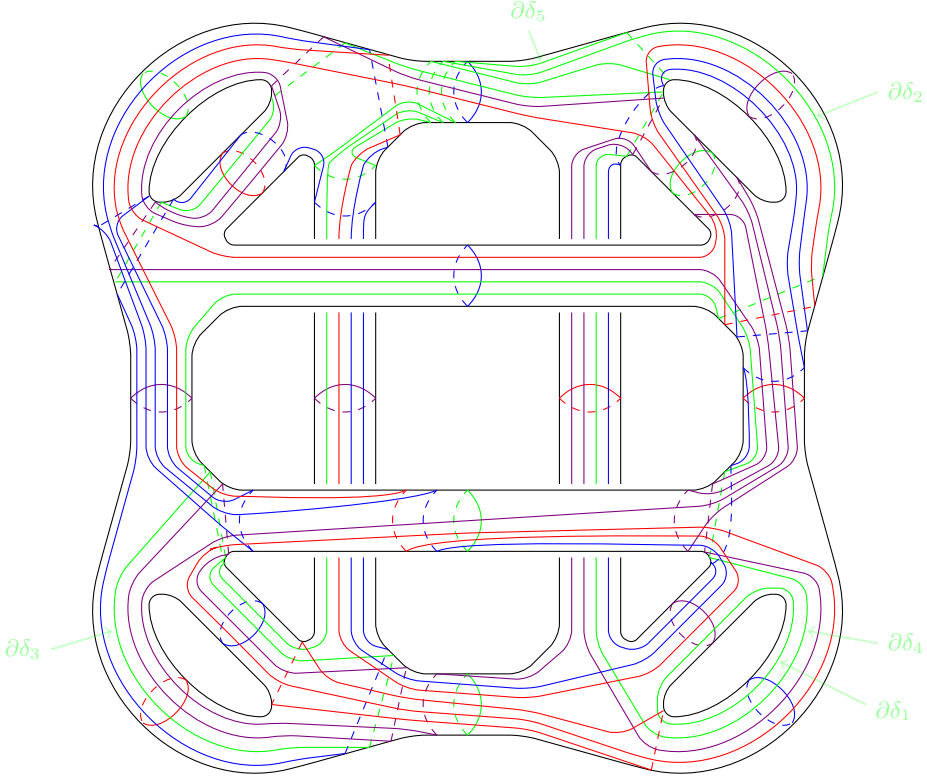

FIGURE 8. Quadrisection diagram for $S^2 \times S^2 \times S^1$.
The cut system representing W_{234}, W_{134}, W_{124}, and W_{123} is in blue, violet, red, and green respectively.

To draw the diagram curves on the genus-9 surface, we need to determine, for each 3-dimensional handlebody of the quadrisection, a family of nine properly embedded disks that cut the handlebody into a 3-ball. We have

$$W_{123} = (M_{123} \times (S^2 \setminus (D_1 \cup D_2 \cup D_3))) \cup (M_{23} \times \partial D_2) \cup (M_{13} \times \partial D_3) \cup (M_{412} \times D_4).$$

From Figure 7, it can be read that M_{23} (resp. M_{13}) is made of two disks, viewed as one bigon and one hexagon regarding the repartition of their boundaries along M_{123} and M_{234} (resp. M_{123} and M_{341}). Our nine disks in W_{123} are as follows (see Figure 9 for the second and third points):

- four meridional disks in the four solid tubes composing $D_4 \times M_{412}$;
- a disk δ_1 obtained as the union of:
  - the product of a point in ∂D_2 and the bigon in M_{23},
  - the product of an arc joining ∂D_1 to ∂D_2 on S^2 and the relevant interval in M_{123} (the one on the boundary of the bigon in M_{23});

- a disk δ_2 obtained as the union of:
  - the product of a point in ∂D_2 and the hexagon in M_{23},
  - the product of an arc joining ∂D_1 to ∂D_2 on S^2 and the three relevant intervals in M_{123};
- disks δ_3 and δ_4 analogous to δ_1 and δ_2 with ∂D_3 instead of ∂D_2 and M_{13} instead of M_{23};
- a disk δ_5 obtained as the product of an arc joining ∂D_1 to itself around ∂D_2 and an interval in M_{123} (different from the ones corresponding to the bigons).

Figure 16 indicates which curves in the diagram represent the boundaries of the five disks δ_i.
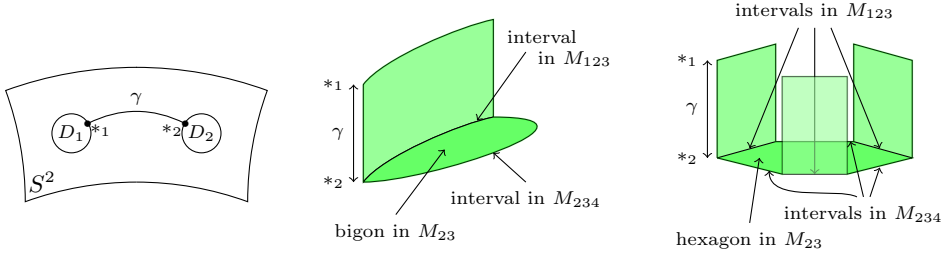

FIGURE 9. Meridional disks in W_{123}.

The other cut systems are obtained similarly. We may note that a simpler quadri-section diagram of $S^2 \times S^2 \times S^1$ is provided in the next section.

We end this section with surface bundles over real projective spaces.

Corollary 3.7. *A surface bundle over $\mathbb{RP}^n$ admits a multisection of genus $2^n g + 2^{n-1}(n-1) + 1$, where g is the genus of the fiber.*

Proof: We need to give a suitable good ball decompositions of $\mathbb{RP}^n$. Using homogeneous coordinates $[x_0 : \cdots : x_n]$ for $\mathbb{RP}^n$, we set $M_i = \{|x_i| \geq |x_j| \mid \forall j\}$. This defines a good ball decomposition of $\mathbb{RP}^n$ where $M_{\{0,\ldots,n\}}$ contains 2^n points and each $M_{\{0,\ldots,n\}\setminus\{i\}}$ is made of 2^{n-1} intervals, for a total of $e = (n+1)2^{n-1}$ intervals. $\square$

4. Multisecting fiber bundles over the circle

For a closed 3-manifold that fibers over the circle, there is a simple construction of a Heegaard splitting, which is the one described in the previous section. It has been generalized to dimension 4 by Gay and Kirby [**2**] and Koenig [**5**]. A similar construction can indeed be performed in any dimension.

Theorem 4.1. *Let W be an $(n+1)$-manifold which fibers over S^1 with fiber a closed n-manifold X and monodromy φ. Assume that X admits a multisection $X = \bigcup_{i=1}^{n-1} X_i$ preserved by φ, meaning that there is a permutation σ of $\{1, \ldots, n-1\}$ such that $\varphi(X_i) = X_{\sigma(i)}$. Then W admits a multisection of genus $(c+n-1)g+1$, where g is the genus of $S = X_{\{1,\ldots,n-1\}}$ and c is the number of cycles in the decomposition of σ (including fixed points as order-1 cycles).*

The following proof generalizes Koenig's proof in dimension 4. In that case, the permutation σ is the identity or a transposition; Koenig indeed obtains a trisection of genus $4g+1$ in the first case and $3g+1$ in the second case. Further, he shows that, in

the case where σ is the identity, some destabilizations can be performed such that one finally ends with a trisection of genus $3g + 1$ in both cases. Similar destabilizations can be performed in some examples in higher dimensions, as in Figures 15 and 16, but we could not find a general argument. It would be interesting to determine whether one can always get a multisection of genus $ng + 1$.

Proof: We construct a multisection of W using the multisection of X and a decomposition of S^1 into intervals. Identifying W with $X \times I/(x,0) \sim (\varphi(x), 1)$, we define the W_i in the product $X \times I$.
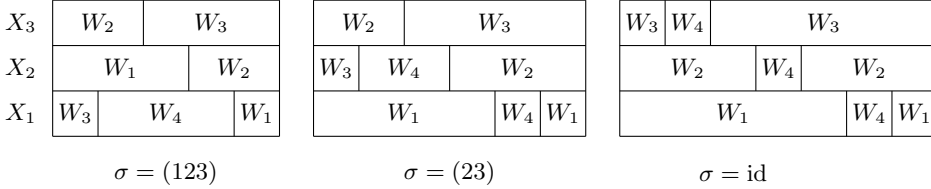
X_3	W_2		W_3	
X_2	W_1		W_2	
X_1	W_3	W_4		W_1

W_2		W_3	
W_3	W_4	W_2	
W_1		W_4	W_1

W_3	W_4	W_3	
W_2		W_4	W_2
W_1		W_4	W_1

$$\sigma = (123) \qquad\qquad\qquad \sigma = (23) \qquad\qquad\qquad \sigma = \mathrm{id}$$

FIGURE 10. Scheme of the quadrisection of W for different permutations σ.

Assume first $n = 4$. There are three cases, depending on the type of σ: identity, transposition, or 3-cycle. These are schematized in Figure 10. For instance, when $\sigma = (123)$, we first set:

$$W_1' = \left(X_1 \times \left[\frac{4}{5}, 1\right]\right) \bigcup_\varphi \left(X_2 \times \left[0, \frac{3}{5}\right]\right), \quad W_2' = \left(X_2 \times \left[\frac{3}{5}, 1\right]\right) \bigcup_\varphi \left(X_3 \times \left[0, \frac{2}{5}\right]\right),$$

$$W_3' = \left(X_3 \times \left[\frac{2}{5}, 1\right]\right) \bigcup_\varphi \left(X_1 \times \left[0, \frac{1}{5}\right]\right), \quad W_4' = X_1 \times \left[\frac{1}{5}, \frac{4}{5}\right].$$

At this stage, the W_i' are handlebodies, but their intersections are not. We shall again fix this by tubing. We say that a 4-ball in X is in *good position* if it is transverse to the X_i, the X_{ij}, and the central surface S, and if it intersects each of these pieces along a ball of the corresponding dimension. Note that such balls do exist: take a small enough neighborhood of a point in the central surface. For each interval in our construction, namely $\left[\frac{i}{5}, \frac{i+1}{5}\right]$ for $i = 1, 2, 3$ and $\left[\frac{4}{5}, 1\right] \cup \left[0, \frac{1}{5}\right]$, we take a tube $B^4 \times I$ made of a 4-ball in good position above each point of the interval, and we add it to the W_i' which does not appear above this interval. For instance, a tube above $\left[\frac{2}{5}, \frac{3}{5}\right]$ is removed from $W_1 \cup W_3 \cup W_4$ and added to W_2' to form W_2. We require distinct tubes to be disjoint.

Let us check that this defines a quadrisection of W. Each W_i is a 4-dimensional handlebody times an interval (namely W_i') connected to itself by a 1-handle, thus a 5-dimensional handlebody. The W_{ij} are made of copies of some X_k and copies of some $X_{k\ell}$ times an interval, joined by two tubes, hence they are 4-dimensional handlebodies; for instance, W_{12} is the union of $X_2 \times \left\{\frac{3}{5}\right\}$ and $\left(X_{12} \times \left[\frac{4}{5}, 1\right]\right) \bigcup_\varphi \left(X_{23} \times \left[0, \frac{2}{5}\right]\right)$ joined by the tubes above $\left[\frac{2}{5}, \frac{3}{5}\right]$ and $\left[\frac{3}{5}, \frac{4}{5}\right]$. The W_{ijk} are made of two copies of some $X_{\ell m}$ and a copy of the surface $S = X_{123}$ times an interval, joined by three tubes. Finally, the central surface $\Sigma = W_{1234}$ is given by four copies of S, above $\frac{i}{5}$ for $i = 1, \ldots, 4$, joined by tubes.

The genera of the surfaces are related by $g(\Sigma) = 4g + 1$, where $g = g(S)$. The schemes of Figure 10 show how to apply this construction for other permutations of the trisection of X. The genus of Σ is then given by $5g + 1$ and $6g + 1$ respectively.

FIGURE 11. Scheme of the multisection of W for a monodromy inducing a cycle.

$n = 6 \qquad \sigma = (12)(345)$

$n = 7 \qquad \sigma = (12)(34)(56)$

FIGURE 12. Other schemes of multisections.

FIGURE 13. Scheme for the permutation $(1 \cdots i_1)(i_1 + 1 \cdots i_2) \ldots (i_{c-1} + 1 \cdots i_c)$.
The blocks in blue, green, and red correspond to the cycles $(1 \cdots i_1)$, $(i_1 + 1 \cdots i_2)$, and $(i_{c-1} + 1 \cdots i_c)$ respectively.

In higher dimensions, the same construction works, as long as we can determine the right scheme. The idea is to use the decomposition of σ into disjoint cycles. Figure 11 gives a model for an $(n-1)$-cycle. Then different cycles can be stacked together

as exemplified in Figures 10 and 12; the general pattern is given in Figure 13. In doing so, we decompose the interval $[0,1]$ into N intervals $I_\ell = \left[\frac{\ell}{N+1}, \frac{\ell+1}{N+1}\right]$ for $\ell = 1, \ldots, N-1$ and $I_N = \left[\frac{N}{N+1}, 1\right] \cup \left[0, \frac{1}{N+1}\right]$; note that N equals the number of cycles in the decomposition of σ (including fixed points as order-1 cycles) plus $n-1$. Also note that, above each interval I_ℓ, $n-1$ distinct W_i's appear (see Figure 13). As above, we first define W_i' as the disjoint union of the $X_k \times I_\ell$ for each interval I_ℓ above which W_i appears in the X_k-line. We say that an n-ball in X is in *good position* if it meets each X_I transversely along a ball. Then, for each interval I_ℓ, we take a tube $B^n \times I_\ell$ made of a ball in good position above each point of I_ℓ, so that the different tubes are disjoint, and we add this tube to the only W_i which does not appear above I_ℓ. This tube is thus removed from the other W_j's; since the trace of the tube on a W_j is a collar neighborhood of a disk in ∂W_j, this amounts to modifying W_j by an isotopy. Thus constructed, the W_i are made of n-dimensional handlebodies times an interval joined by 1-handles, hence they are $(n+1)$-dimensional handlebodies. For a non-empty proper subset I of $\{1, \ldots, n\}$, W_I is made of some $X_J \times I_\ell$ with $|J| = |I|$ and some $X_J \times \left\{\frac{\ell}{N+1}\right\}$ with $|J| = |I| - 1$, joined by 1-handles; hence W_I is an $(n-|I|+2)$-dimensional handlebody. Finally, $\Sigma = W_{\{1,\ldots,n\}}$ is made of N copies of the punctured S joined by N tubes.   □

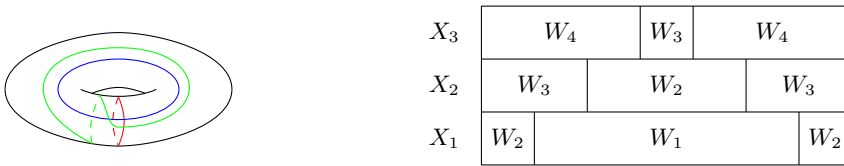| X_3 | W_4 | | W_3 | W_4 | |
| X_2 | W_3 | | W_2 | | W_3 |
| X_1 | W_2 | W_1 | | | W_2 |

FIGURE 14. Trisection diagram for $\mathbb{CP}^2$ and scheme of a quadrisection of $\mathbb{CP}^2 \times S^1$.

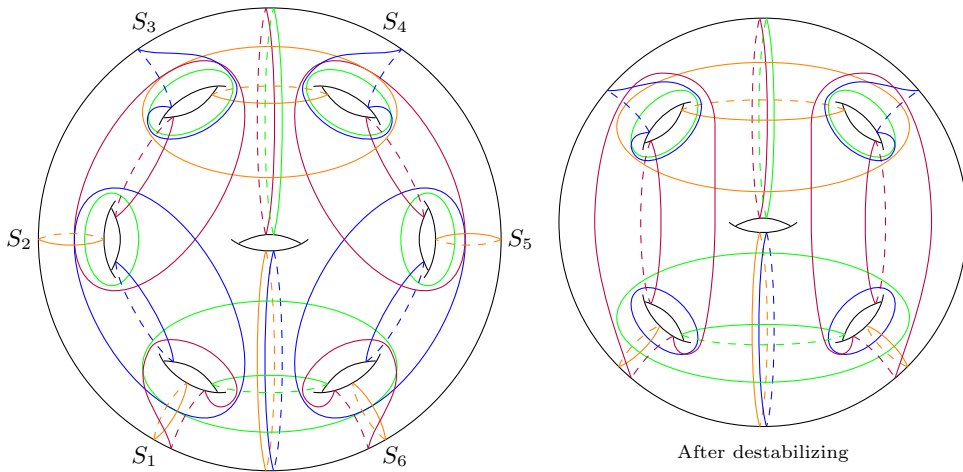FIGURE 15. Quadrisection diagrams of $\mathbb{CP}^2 \times S^1$.

We shall explain on the example of $\mathbb{CP}^2 \times S^1$ how to draw a diagram of the multisection we have constructed. We start with the diagram of $\mathbb{CP}^2$ given on the left hand side of Figure 14, whose surface is denoted by S, where the red curve represents X_{12}, the blue curve represents X_{23}, and the green curve represents X_{13}. We use the alternative scheme given on the right hand side of Figure 14 (this is just for convenience, because a nice picture came out with this scheme). We draw the surface Σ as $N = 6$ copies S_i of S set along a cycle and joined by tubes creating the hole in the middle; see Figure 15. The 3-dimensional handlebodies of the quadrisection are made of copies of the 3-dimensional handlebodies of the trisection of $\mathbb{CP}^2$ and copies of the product of the punctured surface S with an interval, joined by tubes. For instance, in our example, the handlebody W_{124} is made of:

- copies of X_{13} represented by the purple curves on S_1 and S_6,
- the product of a punctured S with an interval running from S_2 to S_3, where the purple curves represent arcs on the punctured S that define disks in the product: here we take any pair of disjoint properly embedded arcs in the punctured S that cut it into a disk, and their product with the interval are disks whose boundaries form a cut system of the associated 2-handlebody,
- the same thing between S_4 and S_5,
- the tubes joining the above pieces, to which corresponds a meridian purple curve which could be drawn between S_i and S_{i+1} for any $i \neq 2, 4$.

The other cut systems are obtained accordingly; the orange one represents W_{123}, the blue one W_{134}, and the green one W_{234}. If the monodromy φ were non-trivial, then the green curves on S_1/S_6 would have to join arcs on S_6 to their images by φ on S_1. Note that we have to represent the successive copies of S with alternating orientation. The monodromy φ reverses the orientation of S precisely when n is odd.

In this diagram, two destabilizations can be performed. Sliding the orange curve on S_2 along the orange curve on S_1 and the green curve on S_2 along the green curve on S_3, we get parallel green and purple curves dual to parallel blue and orange curves. Thanks to Proposition 2.2, this allows us to destabilize once. The second destabilization is symmetric with respect to a vertical axis.

Starting with the genus-2 trisection diagram of $S^2 \times S^2$ given in Figure 16, we get a quadrisection diagram of $S^2 \times S^2 \times S^1$ in a completely analogous manner. In particular, we use the same scheme (see Figure 14) and the same colors. This first gives the genus-13 quadrisection diagram at the top-left of Figure 16. Performing four destabilizations similar to that of Figure 15, we get the genus-9 quadrisection diagram in Figure 16. We can then perform two more destabilizations, which successively merge the pairs of "holes" marked with $*$: at the first step we readily have a pair of parallel blue and purple curves, and we slide some green curves to get the destabilization conditions; at the second step we slide the green curve around the upper $*$-marked hole along the similar green curve on the right, and we slide blue and purple curves to get parallel curves joining the $*$-marked holes. Finally, we get the genus-7 diagram at the top-right of Figure 16.

Note that we obtain a genus-7 quadrisection, which is strictly less than $9 = ng + 1$. This might not be surprising since the last two destabilizations seem to occur by chance more than following a general pattern.
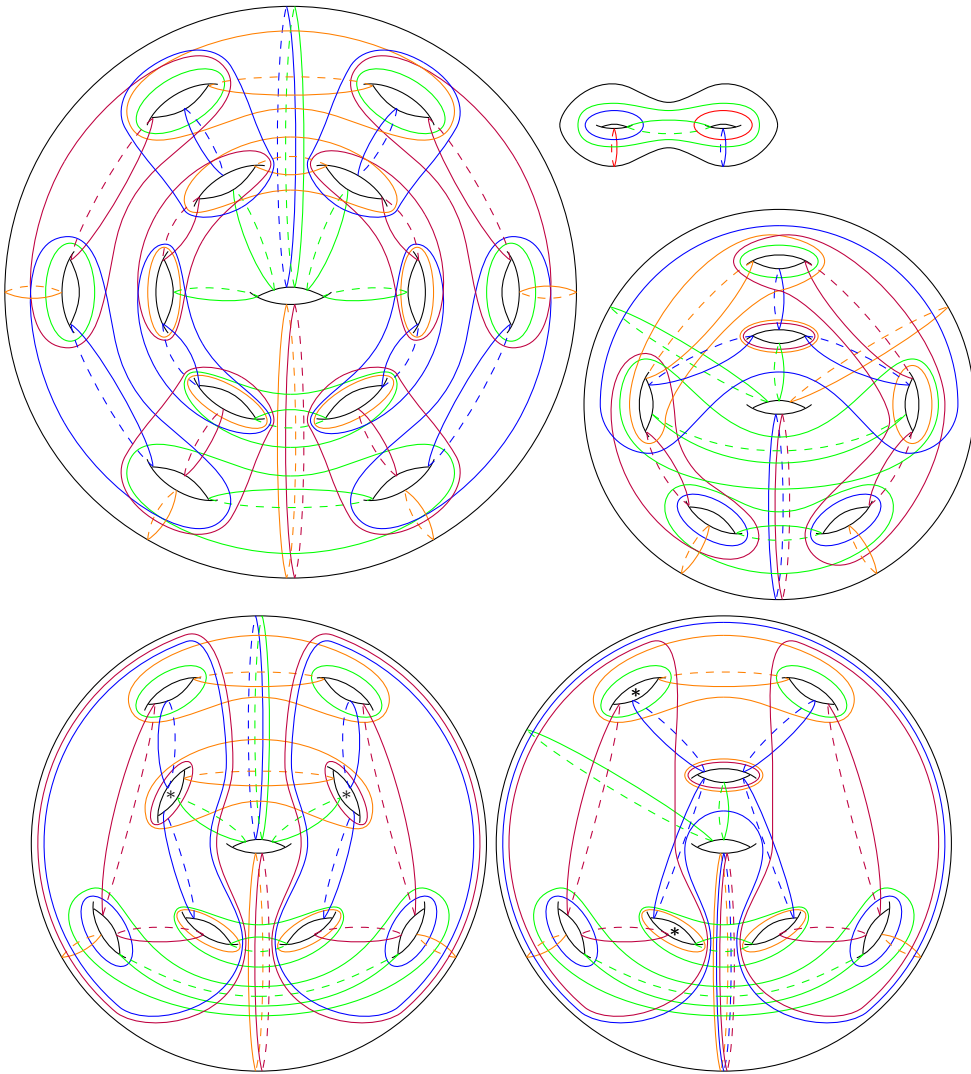
FIGURE 16. Trisection diagram of $S^2 \times S^2$ and quadrisection diagrams of $S^2 \times S^2 \times S^1$.

References

[1] F. BEN ARIBI, S. COURTE, M. GOLLA, AND D. MOUSSARD, Multisections of higher-dimensional manifolds, Preprint (2023). `arXiv:2303.08779`.

[2] D. T. GAY AND R. KIRBY, Trisecting 4-manifolds, *Geom. Topol.* **20(6)** (2016), 3097–3132. `DOI: 10.2140/gt.2016.20.3097`.

[3] G. ISLAMBOULI AND P. NAYLOR, Multisections of 4-manifolds, *Trans. Amer. Math. Soc.* **377(2)** (2024), 1033–1068. `DOI: 10.1090/tran/8996`.

[4] K. JOHANNSON, *Topology and Combinatorics of 3-Manifolds*, Lecture Notes in Math. **1599**, Springer-Verlag, Berlin, 1995. `DOI: 10.1007/BFb0074005`.

[5] D. KOENIG, Trisections of 3-manifold bundles over S^1, *Algebr. Geom. Topol.* **21(6)** (2021), 2677–2702. `DOI: 10.2140/agt.2021.21.2677`.

[6] C. P. ROURKE AND B. J. SANDERSON, *Introduction to Piecewise-Linear Topology*, Reprint, Springer Study Ed., Springer-Verlag, Berlin-New York, 1982. `DOI: 10.1007/978-3-642-81735-9`.

[7] J. H. Rubinstein and S. Tillmann, Multisections of piecewise linear manifolds, *Indiana Univ. Math. J.* **69(6)** (2020), 2209–2239. DOI: 10.1512/iumj.2020.69.8044.

[8] M. Williams, Trisections of flat surface bundles over surfaces, Thesis (Ph.D.)-The University of Nebraska - Lincoln (2020).

Institut de Mathématiques de Marseille (I2M), Centre de Mathématiques et Informatique (CMI), 13453 Marseille Cedex 13, France
E-mail address: delphine.moussard@univ-amu.fr